

# Detection of Glucose in the Human Brain with $^1\text{H}$ MRS at 7 Tesla

Lana G. Kaiser,<sup>1\*</sup> Kawaguchi Hirokazu,<sup>1</sup> Masaki Fukunaga,<sup>2</sup> and Gerald B. Matson<sup>3</sup>

**Purpose:** A new method is proposed for noninvasive detection of glucose in vivo using proton MR spectroscopy at 7 Tesla.

**Theory and Methods:** The proposed method utilizes J-difference editing to uncover the resonance of beta-glucose ( $\beta$ -glc) at 3.23 ppm, which is strongly overlapped with choline. Calculations using the density matrix formalism are used to maximize the signal-to-noise ratio of the  $\beta$ -glc resonance at 3.23 ppm. The calculations are verified using phantom and in vivo data collected at 7 Tesla.

**Results:** The proposed method allows observation of the glucose signal at 3.23 ppm in the human brain spectrum. Additional co-edited resonances of N-acetylaspartylglutamate and glutathione are also detected in the same experiment.

**Conclusion:** The proposed method does not require carbon ( $^{13}\text{C}$ )-labeled glucose injections and  $^{13}\text{C}$  hardware; as such, it has a potential to provide valuable information on intrinsic glucose concentration in the human brain in vivo. **Magn Reson Med** 76:1653–1660, 2016. © 2016 International Society for Magnetic Resonance in Medicine

**Key words:** MRS; glucose; 7 Tesla; jedit-SLASER; numerical simulations; human brain

## INTRODUCTION

Glucose serves as the primary energy source in the mammalian brain (1). Direct and indirect glucose measurements in vivo are possible using NMR imaging and spectroscopy due to the unique spectroscopic properties of glucose (2,3). Both direct carbon ( $^{13}\text{C}$ ) and indirect  $^{13}\text{C}$ -proton ( $^1\text{H}$ ) magnetic resonance spectroscopy (MRS) utilizing  $^{13}\text{C}$  infusions have been used to study various important metabolic pathways, including the tricarboxylic acid cycle and glycolysis (4,5). As such,  $^{13}\text{C}$  MRS can serve as a dynamic marker of brain glucose changes following a labeled glucose infusion. However, information about intrinsic glucose concentrations in brain tissue is not accessible via  $^{13}\text{C}$  MRS measurements. In contrast,  $^1\text{H}$  MRS has the potential to detect natural in vivo glucose

distribution without invasive injections. Furthermore, it is not limited by the complicated additional requirements of  $^{13}\text{C}$  channel hardware/pulse sequences.

The main challenge for the use of  $^1\text{H}$  MRS for glucose detection is due to the low natural concentration of glucose and spectral overlap with higher concentration metabolites/water resonance. Therefore, existing  $^1\text{H}$  MRS methods also utilize glucose infusions (6–8). For the two configurations (anomers) of glucose, alpha ( $\alpha$ -glc) and beta ( $\beta$ -glc) (occurring in vivo with an approximate 36:64 ratio (9)), only a resonance of  $\alpha$ -glc at 5.23 parts per million (ppm) is relatively separated from other peaks. Gruetter et al. (6,10) demonstrated quantification of this resonance with  $^1\text{H}$  MRS in human brain *in vivo* at 4 Tesla (T) using an ultrashort echo time (TE) STEAM sequence. A disadvantage of this method is that almost a factor of 4 in signal intensity is lost due to the inherent STEAM method (a factor of two) and the fact that the  $\alpha$ -glc anomer is present in only half of quantity of  $\beta$ -glc. Furthermore, the 5.23 ppm resonance is relatively close to the intense water resonance at 4.7 ppm, even at higher magnetic fields. Therefore, this method relies on excellent shimming, highly optimized water suppression, and complete elimination of unwanted coherences around the suppressed water region. Even when these conditions are satisfied, a variable baseline due to the residual water signal complicates the direct quantification of glucose from short TE spectra (11). Another strategy for glucose detection is based on multiple quantum filtering, as first shown by Keltner et al. (12). This method detected a combination of  $\alpha$ -glc and  $\beta$ -glc spectral signals in the region at  $\sim 3.8$  ppm; however, despite relatively high signal intensity, it suffered from large overlap with other metabolites. More recent experiments rely on detection of  $\beta$ -glc at 4.63 ppm via either multiple quantum coherence editing (13) or localized Total Correlated Spectroscopy (7). The advantage of these methods is that the more abundant  $\beta$ -glc anomer is detected, and these methods comprise a single shot acquisition. The disadvantage is that about half of the signal is lost due to the inherent mechanism of the multiple quantum filter, and the spectral quantification is more challenging. We are not aware of the use of the  $\beta$ -glc resonance at 3.23 ppm for the detection of glucose, and in general of the use of a J-difference editing method for the detection of glucose.

The main goal of this study is to investigate the detection of a  $\beta$ -glc resonance at 3.23 ppm using a J-difference editing technique at 7T. Higher field (e.g., 7T) spectroscopy provides increased sensitivity and better frequency

<sup>1</sup>Siemens Healthcare KK, Tokyo, Japan.

<sup>2</sup>National Institute for Physiological Sciences, Okazaki, Aichi, Japan.

<sup>3</sup>University of California, San Francisco, California, USA.

Grant sponsor: Supported by Siemens Healthcare KK in Tokyo, Japan.

\*Correspondence to: Lana G. Kaiser, Siemens Healthcare K.K., Japan, Gate City Osaka West Tower, 1-Chome 11-1, Shinagawa-ku, Osaka, Tokyo 141-8644, Japan. E-mail: lana.kaiser@siemens.com.

Received 7 April 2016; revised 12 August 2016; accepted 15 August 2016  
DOI 10.1002/mrm.26456

Published online 8 September 2016 in Wiley Online Library (wileyonlinelibrary.com).

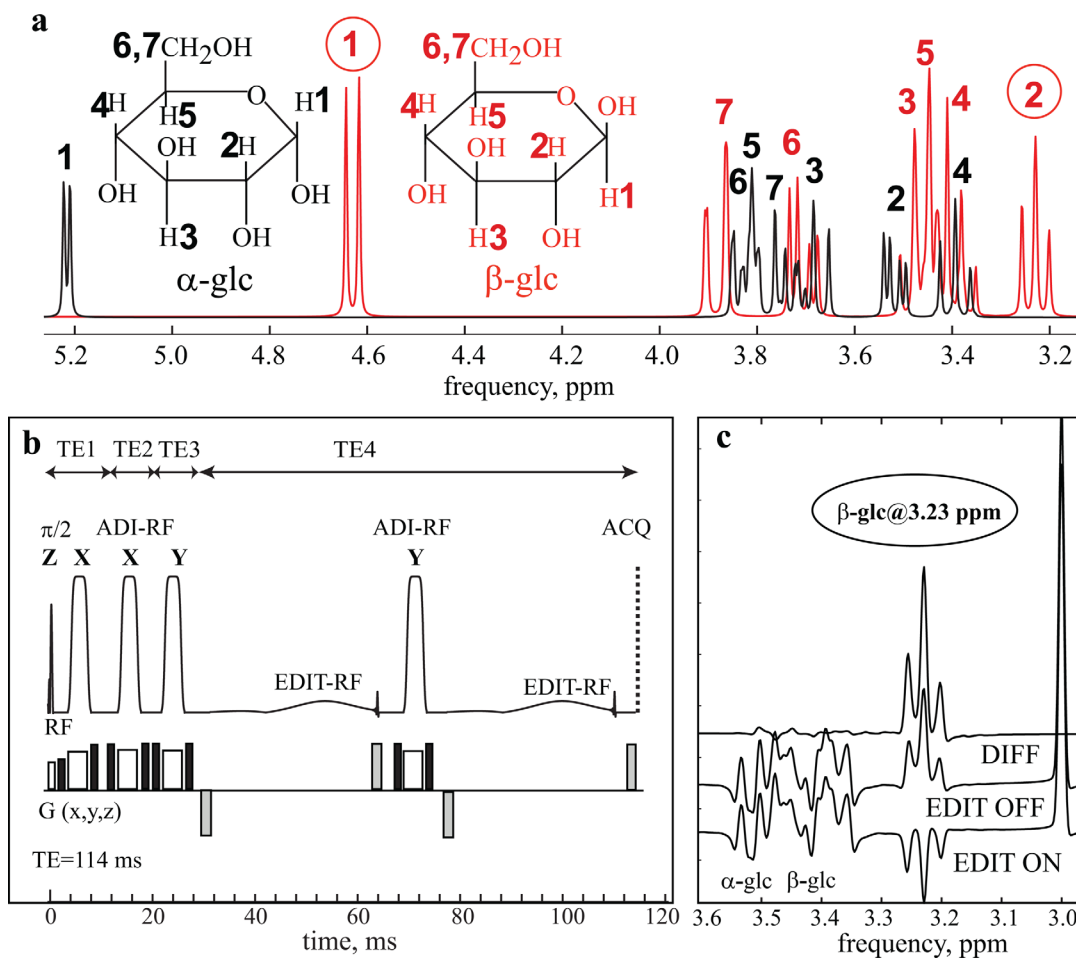


FIG. 1. (a) A simulation of  $^1\text{H}$  MR spectra of the glucose anomers at 7 Tesla (pulse-acquire sequence). The targets of the proposed J-editing method (protons H<sub>1</sub> and H<sub>2</sub> of  $\beta$ -glc) are designated with red circles. The difference between  $\alpha$ -glc and  $\beta$ -glc is the axial versus equatorial orientation of -OH group at a position of H<sub>1</sub> relative to the CH<sub>2</sub>OH group. (b) Optimized asymmetric arrangement of editing and slice-selective RF pulses in SLASER (TE = 114 ms, TE<sub>1</sub> = 11 ms, TE<sub>2</sub> = 8.5 ms, TE<sub>3</sub> = 8.5 ms, TE<sub>4</sub> = 86 ms). During the EDIT ON scan, editing RF pulses are centered on  $\beta$ -glc resonance at 4.63 ppm. For the EDIT OFF scan, editing pulses are centered at 7.5 ppm. In addition to asymmetric locations relative to the center of the timing diagram, asymmetric editing RF pulse shapes (minimum phase) were used for further signal intensity enhancement. These RF pulses were used in combination with bipolar gradients (gray). (c) Simulated glucose spectra obtained using the sequence components and timing parameters of the asymmetric jedit-SLASER sequence. A singlet peak from one proton at 3 ppm is added as a relative signal-intensity reference.

separation. Although J-difference MRS *in vivo* is mostly performed using the MEGA-PRESS sequence (14), higher B<sub>0</sub> field necessitates alternative approaches due to B<sub>1</sub>-related artifacts. Semi-LASER (SLASER) localization has been shown to overcome some of the artifacts at 7T, such as high B<sub>1</sub> inhomogeneity and limited B<sub>1</sub> power (15). In this work, SLASER is used for localization in combination with two narrow frequency-band-selective pulses for J-editing. The original MEGA scheme implies execution of water suppression using dual-band editing pulses (in case of J-editing) and a specific crusher gradient arrangement (which utilizes one slice-selective 180-degree pulse to achieve total dephasing of unwanted coherences) (14). However, our goal is to invert 4.63 ppm resonance of  $\beta$ -glc; therefore, it is not possible to utilize the MEGA scheme as it was originally designed. Furthermore, our arrangement proposed here uses a different

gradient scheme (16) with bipolar gradients around editing radiofrequency (RF) pulses; therefore, we simply refer to the technique as jedit-SLASER.

## THEORY

There are seven protons in the  $\alpha$ -glc and  $\beta$ -glc anomers, giving rise to a complex spectral pattern from 14 protons (Fig. 1a). The  $\beta$ -glc resonances at 3.23 ppm arise from the H<sub>2</sub> proton, which is coupled to the H<sub>1</sub> proton at 4.63 ppm with a  $J_{12}$  = 8.0 Hz, and to the H<sub>3</sub> proton at 3.47 ppm with  $J_{23}$  = 9.1 Hz (17). Thus, although the H<sub>2</sub> proton appears as a triplet with J coupling of  $((8.0 + 9.1)/2)$  = 8.55 Hz, it is actually a doublet of doublets. At 7T, the frequency separation between the H<sub>2</sub> and H<sub>3</sub> protons is 73 Hz, but between the H<sub>2</sub> and H<sub>1</sub> protons it is 420 Hz. Thus, the coupling is designated as ABX (18). For a

simple spin echo experiment (EDIT OFF) with a TE of 117 ms, the apparent triplet would be expected to be upright; however, for the EDIT ON scan, where the coupling to the  $H_1$  proton is effectively removed, the  $H_2$  proton would evolve during the TE time as a doublet with a  $J=9.1$  Hz. During acquisition, all J-coupled evolution is active; thus, the  $H_2$  proton should appear roughly as an inverted triplet for TE=117 ms.

The actual experiment is complicated by the fact that the spin system is an ABX system with slightly unequal coupling constants ( $J_{AB}=8.0$  Hz,  $J_{AX}=9.1$  Hz), and the J-evolution due to  $J_{AB}$  coupling is altered by the spin echo pulses. In the optimized experiment, the excitation and first three spin echo pulses are spaced as closely together as possible, consistent with allowing time between RF pulses for required gradient pulses. Thus, the first pulses operate as a multiple spin echo sequence with timings of  $t1/2=5.50$  ms,  $t2/2=4.20$  ms, and  $t3/2=4.30$  ms (corresponding to TE1=11 ms, TE2=8.5 ms). As a result, this part of the sequence operates approximately as a Carr-Purcell sequence with a spin-echo pulse spacing  $t_{CP}$  of just over 9 ms.

Allerhand (19), Eq. 58a, shows that for small  $J/\Delta\delta$  (8 Hz/73 Hz, where  $\Delta\delta$  is the frequency separation between the J-coupled resonances), the phase evolution of the AB coupled spin is reduced by the factor  $1 - \sin(R_{\tau}/2)/(R_{\tau}/2)$ , where  $\tau$  is the time between spin echo pulses, and  $R=2\pi\sqrt{J^2+\Delta\delta^2}$ . Using Allerhand's results, we expect the effect of  $J_{AB}$  to be reduced by roughly a factor of 0.6 at the time of the echo occurring just past 28 ms, where time zero is the center of the excitation pulse.

In this approximate analysis, for the EDIT OFF experiment an outer-line phase evolution for the first 28 ms is at  $(9.1 \cdot 0.6 + 8.0)/2$  Hz, whereas an inner line evolution is at  $(9.1 \cdot 0.6 - 8.0)/2$  Hz, yielding outer lines at  $\pm 68$  degrees and inner lines at  $\pm 13$  degrees. For the duration of the EDIT OFF sequence, the outer lines evolve at  $(9.1 + 8.0)/2$  Hz and the inner lines at  $(9.1 - 8.0)/2$  Hz. In this approximate analysis, the outer lines would be upright at 28 ms + 95 ms = 123 ms, whereas the inner lines would be upright and coalesced at 28 ms + 66 ms = 94 ms. Because the outer lines are evolving much faster than the inner lines, this analysis suggests that the optimal TE for the EDIT OFF experiment should be close to 120 ms. For the EDIT ON experiment, if the phase evolution due to  $J_{AX}$  is fully suppressed, this analysis suggests that the observed multiplet would be inverted at TE of  $1/8.0=125$  ms. Finally, simulations did not include losses due to  $T_2$  relaxation but were performed with the fact in mind that, other things being equal, a shorter TE time was to be preferred. In addition to  $T_2$  considerations, the choice of the overall optimal TE time in our method is skewed toward the optimum TE time of the central peak of the triplet (TE=94 ms) rather than the outer lines (TE=123 ms).

The analysis based on Allerhand's formulas uses ideal pulses; therefore, numerical simulations using actual experimental RF pulse shapes are needed to further refine the optimum timings for the experiment (divided into 4 subecho times in jedit-SLASER experiment). Previously, numerical simulations utilizing real

experimental components were shown to be successfully utilized for creating model data basis sets for accurate quantification (20). Similar calculations were also used to develop an optimized editing  $^1H$  MRS method for maximum signal-to-noise ratio (SNR) gain of the  $\gamma$ -amino butyric acid (GABA) signal at 3 ppm (21). In this work, the final optimized sequence for  $\beta$ -glc detection based on the numerical simulations is presented here with confirmation from phantom and in vivo data.

## METHODS

All data was collected on a 7T Magnetom system (Siemens, Erlangen, Germany) with maximum gradient strength=70 mT/m. A circular polarized transmit coil from Nova Medical Inc. (Wilmington, MA) with integrated 32 receive channels was used for all data acquisition. Localization was based on the images generated by magnetization-prepared two rapid gradient echoes (MP2RAGE) sequence (22). A 27 mL ( $3 \times 3 \times 3$  cm<sup>3</sup>) voxel was selected in sagittal midline above the corpus callosum. The available  $B_1$  *in vivo* for this specific voxel location was approximately 25 microtesla. Prior to the metabolic data acquisition, the voxel was shimmed using a combination of the standard Siemens automated localized shimming procedure, followed by manual shimming. This resulted in a linewidth of 10 Hz for water, and of 8 Hz for N-acetylaspartate (NAA) (full-width half-maximum [FWHM]) in the *real* or phased mode of the spectra. The phantom was prepared with a phosphate-buffered saline sachet for the buffering action (pH=7.3). The temperature of the solution at the time of the scan was  $36 \pm 5^\circ\text{C}$ . The same concentration of glucose and acetate (50 mM) was used for the phantom.

All RF pulses for the proposed jedit-SLASER sequence were designed using MATPULSE software (23) based on MatLab software (MathWorks, Natick, MA). This pulse sequence contained four slice-selective adiabatic hypersecant RF pulses (4.5 ms) and two minimum phase editing RF pulses (33 ms). The bandwidths of the volume-selective and -editing RF pulses were 5.5 kHz and 55 Hz (FWHM of inversion profile), respectively. The first excitation 90-degree pulse was 1.6 ms long (bandwidth=4 kHz, FWHM), with an asymmetric minimum phase shape. In vivo MRS data parameters were TE=114 ms (with 4 subecho times: TE1=11 ms, TE2=8.5 ms, TE3=8.5 ms, TE4=86 ms), TR=6 s, and total number of averages=128 (EDIT OFF=64 scans, EDIT ON=64 scans). The total acquisition time was 12.8 minutes. Acquisition spectral width was 6 kHz, with 4,096 points (real) in the collected free-induction decay. Outer volume suppression (OVS) was not used in the sequence. Phantom data was collected with parameters identical to in vivo data, except that 32 total averages were used. In both cases, unsuppressed water reference spectra were acquired for overall phase correction, eddy current compensation, and receive channel reconstruction. Spectral processing for the in vivo/phantom data consisted of correcting the data for multiple channel phase/intensity variations, followed by zero-filling, Gaussian broadening of 3 Hz, and Fourier transform using in-house-designed MatLab (MathWorks)-based software.

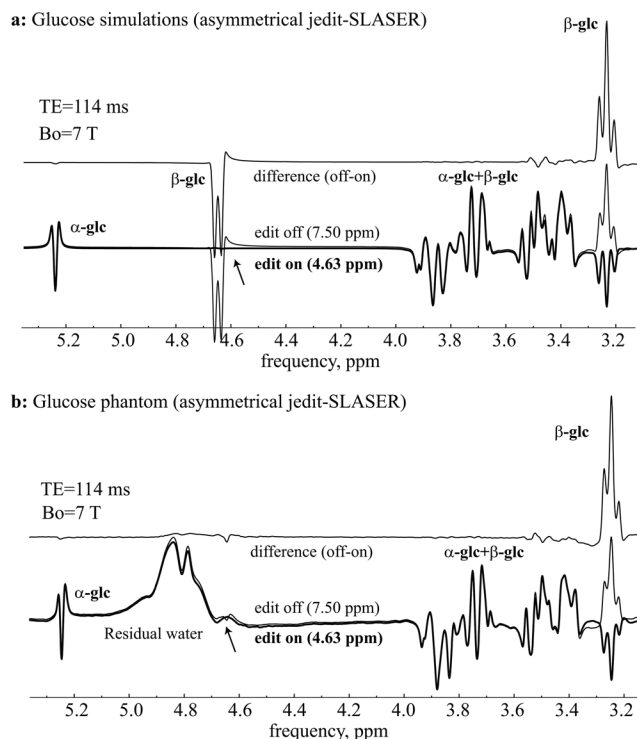


FIG. 2. Validation of the proposed optimized J-difference asymmetrical jedit-SLASER method using numerically simulated data (a) and a glucose phantom solution (b). During the EDIT ON scan (bold), a narrow inversion band editing pulse is centered at 4.63 ppm (in the EDIT OFF scan, it is centered at 7.50 ppm). Apart from small eddy current- and water suppression-induced spectral distortions, the simulated spectra are in good agreement with phantom results.

Numerical simulations using density matrix theory were performed similar to the procedure outlined previously (20,24). The calculations for this study were performed on a personal computer, without the use of parallel processors, due to the improved efficiency of the computational algorithms (25).

In vivo spectra were collected using two male subjects. The subject participated after giving informed consent according to procedures approved by the local institutional review board committee. No glucose infusions were used. About 20 minutes before the data acquisition, the first subject (29 years old) drank a can of white peach juice (350 mL, containing 39 grams of sugar) from Sapporo Fuji House, Sapporo, Japan. The labeling did not specify the specific composition of the sugar (e.g., fructose or glucose). The second subject (29 years old) had lunch approximately 1 hour before the scan and no juice before the scan.

## RESULTS

Figure 1b shows a timing diagram of optimized jedit-SLASER sequence arrangement for detection of  $\beta$ -glc resonance at 3.23 ppm at 7T. This is a result of simulating various combinations of localization/editing RF pulses to achieve an optimum combination for the highest SNR for the difference spectrum. This arrangement is different from the MEGA-SLASER sequence previously

demonstrated for GABA detection at 7T (26). MEGA-SLASER (or any generic jedit-SLASER) for weakly coupled spin systems such as GABA or lactate is optimally arranged with three closely spaced 180-degree pulses in the middle of the sequence, at approximately TE/2, with the two editing pulses arranged symmetrically around the three 180-degree pulses. For such cases, during the EDIT ON scan the J-evolution is divided into two symmetrical time periods based on the editing RF pulse locations. At the end of EDIT ON scan, if sequence timings are carefully optimized, a spectral pattern due to J-evolution approaches the case of TE = 0 or no J-evolution (e.g., for the GABA spin system). In principle, this type of pulse sequence is appropriate for glucose J-difference editing as well; however, it is not optimal. The strong J-coupling of the  $\beta$ -glc H<sub>2</sub> proton and relatively short time spacing between 3 RF slice selective pulses (see Theory section) necessitates a different SLASER scheme, which is described in Figure 1b. In addition to creating J-refocusing asymmetry with respect to the total TE evolution by virtue of their positioning, the editing RF shapes themselves were also created to be asymmetrical (minimum phase shape). In such arrangement, the editing pulses are arranged to optimize the EDIT ON experiment. Optimum TE, TE<sub>1</sub>, TE<sub>2</sub>, TE<sub>3</sub>, and TE<sub>4</sub> periods were calculated to be 114, 11.0, 8.5, 8.5, and 86 ms, respectively. Figure 1c demonstrates a result of the numerical simulation of the proposed editing sequence. During the EDIT ON scan, selective inversions were applied at 4.63 ppm (at a spectral location of the coupling partner at 3.23 ppm). During the EDIT OFF scan, selective inversions were applied at 7.50 ppm, which allows uninterrupted J-evolution. The difference spectrum (OFF-ON) contains  $\beta$ -glc resonance at 3.23 ppm; in a nonedited in vivo spectrum, this resonance is always overlapped by the intense glycylphosphorylcholine and phosphorylcholine signals. The simulated resonance of one singlet spin <sup>1</sup>H at 3 ppm is used as a total signal intensity reference because the <sup>1</sup>H  $\beta$ -glc apparent triplet peak is also due to one spin, <sup>1</sup>H.

Figure 2 demonstrates a comparison of the optimized glucose simulations spectra (a) against phantom data collected at 7T (b). Figure 2a shows the simulations of EDIT ON (bold), EDIT OFF, and the difference spectrum using the asymmetrical jedit-SLASER sequence (TE = 114). The simulations for Figure 2a were performed separately for  $\alpha$ -glc and  $\beta$ -glc and were combined with 0.36:0.64 ratio, respectively. Figure 2b shows the same data from the phantom solution. The simulations are in good agreement with experimental phantom data. Apart from the vanished resonance at 4.63 ppm in the EDIT ON spectrum (due to water suppression) and small eddy current distortions, the spectral pattern is well matched in all spectral positions of both  $\alpha$ -glc and  $\beta$ -glc spectra. This also validates the glucose chemical shifts and J-values under physiological pH and temperature obtained by Govindaraju et al. (17). There was only one minor change in J-value of  $\beta$ -glc (coupling of H<sub>5</sub> and H<sub>6</sub>) protons (changed from 1.6 to 2.27 Hz) for the simulations in Figure 2a. This updated value (2.27 Hz) was reported in a different report of glucose J values and chemical shifts (27), and it agrees better with the phantom data. But this



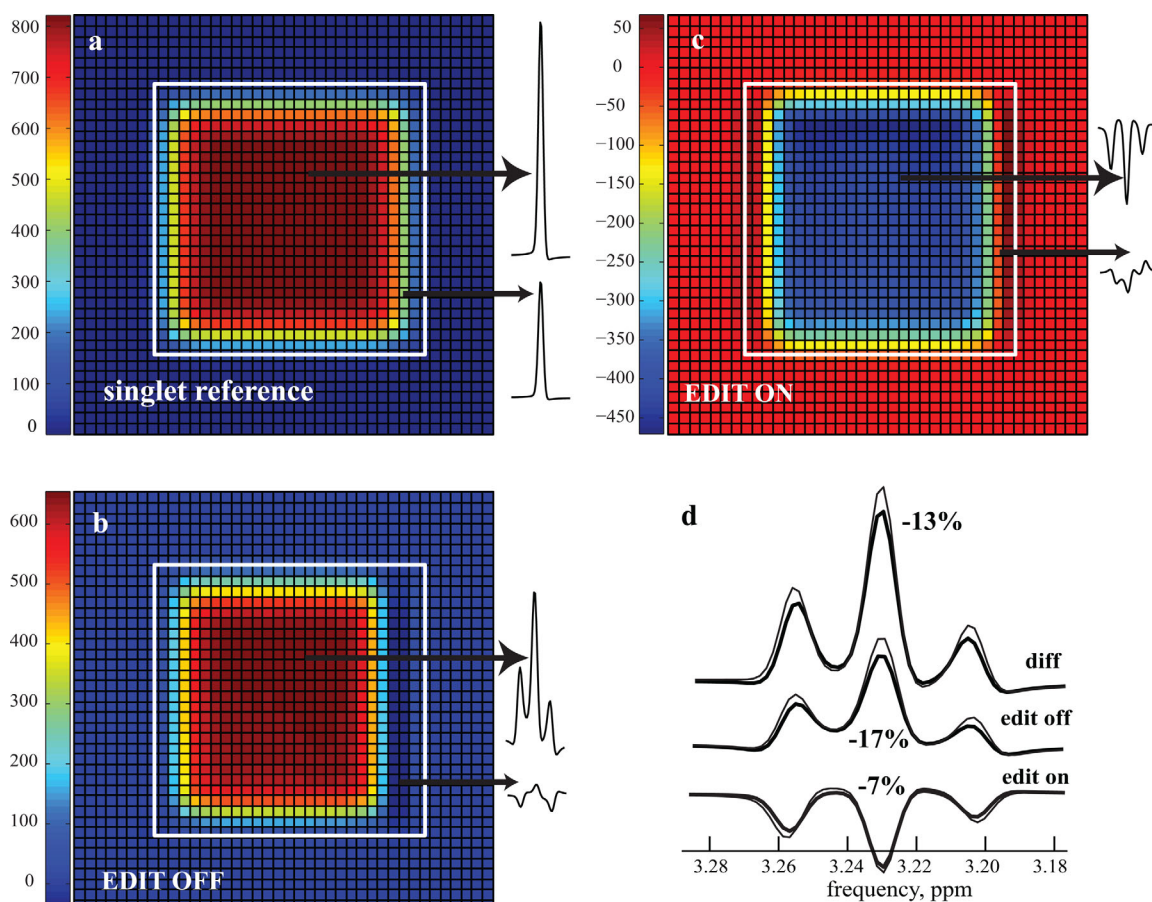


FIG. 3. 2D spatial localization of  $\beta$ -glc resonance at 3.23 ppm based on numerical simulation of the proposed asymmetrical jedit-SLASER scheme (with 4 adiabatic RF pulses). A fictitious singlet resonance of one proton at 3.23 ppm (a) is used as a reference. The EDIT OFF scan simulation (b) shows a distinct compartment on the right side of the voxel, which contributes a small amount of negative intensity (for the outer peaks of the pseudo-triplet). The EDIT ON simulation (c) shows two compartments (right-hand and left-hand sides) that also contribute a small amount of opposite phase compared to the central location of the voxel. The summed spectra (d) from the EDIT OFF, EDIT ON, and difference (EDIT OFF–EDIT ON) scans (bold line) are compared to spectra from the middle of the 2D slice (thin line). The total signal loss in the difference spectrum was calculated to be 13%.

change does not affect the appearance of the main target peak of  $\beta$ -glc at 3.23 ppm, which originates from  $H_2$  proton.

Figure 3 shows a two-dimensional (2D) spatial localization distribution of the  $\beta$ -glc resonance intensity based on numerical simulation of the proposed asymmetrical jedit-SLASER scheme. The results are shown with reference to a fictitious singlet resonance of one proton spin at 3.23 ppm (Fig. 3a). Although singlets do not experience signal loss via the chemical shift displacement (CSD) artifact (21), J-coupled resonances at longer TE can lose a substantial amount of signal, especially at a higher field. Figure 3b and 3c show 2D slices selected by the four adiabatic RF volume-selective pulses, with signal intensity represented by the integrated area of the triplet peak for EDIT OFF and EDIT ON scans, respectively. Figure 3d shows total summed spectra of  $\beta$ -glc EDIT ON, EDIT OFF, and difference at 3.23 ppm (bold) and spectra from the center of the slice (thin). The relative intensity ratio was calculated using the fictitious singlet reference peak-total summed spectrum divided by the spectrum from the center of the slice. The results show that the

EDIT OFF scan (Fig. 3b) contributed the most to the signal loss, amounting to approximately 17% intensity reduction. The EDIT ON scan (Fig. 3c) contributed less, resulting in 7% loss. Overall, the contribution of the CSD artifact was calculated to be 13% (Fig. 3d, top) in the J-difference spectrum. The arrangement order of the 180 pulses presented in Figure 3 was X-X-Y-Y (referring to the direction of the gradient selection). An alternative arrangement of X-Y-Y-X was also explored and yielded a slightly larger signal loss amounting to 16%. The calculated signal loss is attributed to the finite bandwidth (5.5 kHz) of the slice-selective adiabatic RF pulses. The calculated signal loss needs to be accounted for in a quantification routine if the fitting procedure does not use localized model spectra.

Figure 4 shows the application of the proposed asymmetrical jedit-SLASER method for glucose detection in vivo. Figure 4b shows voxel (27 mL) placement location in the parietal lobe above corpus callosum, using MP2RAGE high-resolution images. Figure 4a shows experimental in vivo spectra ranging from 1 to 5.5 ppm at TE = 114 ms. The EDIT ON scan (4a, middle) shows

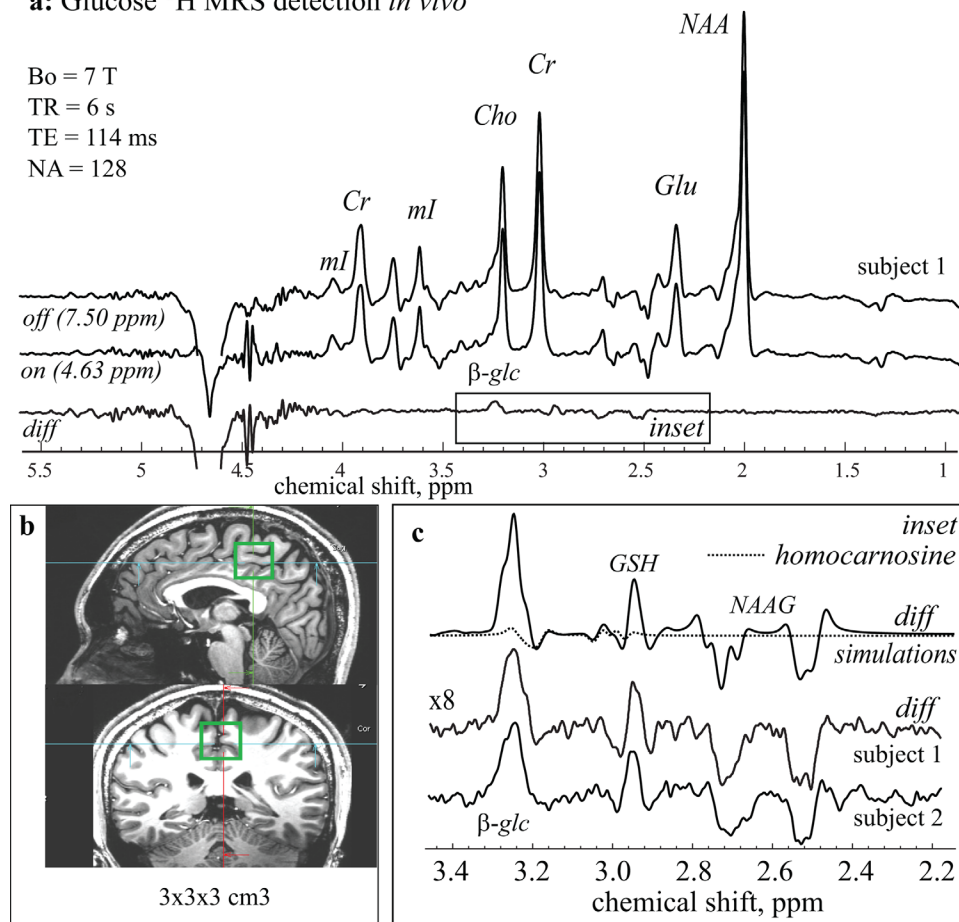
**a: Glucose  $^1\text{H}$  MRS detection *in vivo***

FIG. 4. Demonstration of the asymmetrical jedit-SLASER sequence performance ( $TE = 114\text{ ms}$ ) for glucose detection *in vivo*. (a) EDIT ON scan (middle) with editing RF pulses centered at 4.63 ppm. The EDIT OFF scan (top) is a result of the editing RF pulse centered away from glucose resonances (7.5 ppm). The difference spectrum (bottom) shows four distinct peaks in the range between 2 and 3.8 ppm (assigned to  $\beta$ -glc, GSH, and NAAG). (b) Voxel (27 mL) placement location above the corpus callosum. The inset (c) shows a zoomed-in region (increased vertically by a factor of 8) for final *in vivo* difference spectrum and a corresponding simulation. The simulation used intensity scaling factors of 3:1:2 for  $\beta$ -glc, GSH, and NAAG, respectively. The homocarnosine (dotted line) was calculated to contribute about 5% of overall signal intensity at 3.23 ppm (assuming homocarnosine of the same concentration as glucose).

almost complete water suppression due to the editing RF pulse centered at 4.63 ppm (which is flanked by two dephasing gradients of opposite signs). The area around the water suppression region, including the location of the previously detected the  $\alpha$ -glc at 5.23 ppm, shows some undesired spectral distortions/contributions that are most likely due to insufficient shimming and lack of OVS. Both shimming and optimized OVS are difficult to carry out at 7T. This underscores the challenge of trying to quantify  $\alpha$ -glc peak at 5.23 ppm. On the other hand, the spectral region between 1 ppm and 3.9 ppm is much less affected by unwanted coherences. The inset (Fig. 4c) shows a zoomed-in region (increased vertically by a factor of 8) for the final difference spectrum. This inset also contains numerical simulations of the difference spectrum for comparison. The simulations used all known metabolites above 0.1 mM concentration *in vivo* that had the potential of being affected by the proposed jedit-SLASER editing scheme (e.g., spectral location of J-coupled resonance within 4.55–4.7 ppm). The resultant species affected

by the editing pulse (in addition to the target resonance of  $\beta$ -glc at 4.63 ppm) were the cysteine residue of glutathione (GSH), N-acetylaspartylglutamate (NAAG), and homocarnosine. The latter is considered to be an unwanted co-edited contribution because it resonates at 3.2 ppm, similar to target resonance of  $\beta$ -glc. If we assume a 1:1 concentration ratio of homocarnosine to glucose (which is most likely an overestimation) for the simulations, then the homocarnosine contributes to about 5% of overall signal intensity at 3.23 ppm (dotted line). The other co-edited resonances of GSH and NAAG are not overlapped with the target  $\beta$ -glc signal and therefore can be considered an additional bonus to this method.

The difference spectrum was used for spectral fitting of the  $\beta$ -glc peak, with both Lorentzian and Gaussian line shapes. The EDIT OFF spectrum was used for fitting the creatine (Cr) (total) resonance, with model spectra containing two resonances (creatine and phosphocreatine). Assuming identical T2 relaxation rates for both Cr (total) and  $\beta$ -glc, and concentration of Cr (total) of

10 mM (6),  $\beta$ -glc concentration was calculated to be 1.7 mM. Because  $\beta$ -glc comprises about 0.64 of the total glucose, we estimate a total glucose concentration of 2.7 mM. This value is higher than the normal range of previously reported glucose concentration in vivo (9), probably due to a juice drink (subject 1) or lunch (subject 2) taken before the scan. Blood plasma glucose levels fluctuate hourly, showing a distinct spike after a meal or ingestion of a sugar-containing drink. Because glucose is taken across the blood–brain barrier by transporters, the increase in glucose concentration in neuronal cells is expected. Further work with better control of human subject food/drink intake is needed, where fasting time and amount of glucose taken orally prior to the MR scan is known.

## DISCUSSION

The method presented here does not require  $^{13}\text{C}$ -labeled glucose injections and  $^{13}\text{C}$  hardware to observe glucose in vivo. The editing efficiency suffers from virtually no signal loss in the difference spectrum, similar to J-difference lactate editing, despite being an apparent triplet. Unlike GABA editing, which focuses on a triplet peak at 3.0 ppm, the entire triplet pattern of  $\beta$ -glc is inverted during editing, not just the outer peaks. This contributes to almost complete preservation of the signal in the final difference spectrum. This method is also suitable for use at 7T with symmetric MEGA-SLASER localization, as previously demonstrated for GABA (26). In fact, this type of arrangement was used as a starting point for optimization in this study. However, the symmetric sequence also needs to be optimized specifically for different total TE and RF pulse spacing. Our simulations (out of scope of this article's goal) show that using TE = 114 in a symmetric sequence is largely suboptimal. The details of such calculations will be presented in the future work. Our simulations using different types of SLASER arrangements for the J-difference method presented here indicate that the  $\beta$ -glc J-difference method will work in principle anywhere between TE = 90 and 125 ms. However SNR yield of the J-difference spectrum will vary significantly depending on the specific parameters within the SLASER-based localization sequence. The numerical computer simulations indicated an optimal TE time of around 114 ms for the asymmetric jedit-SLASER sequence, which is consistent with the rationale outlined in the Theory section. The pseudo-triplet pattern of glucose at 3.2 ppm makes a good detection target using the proposed method for the field strengths of 4T and higher. Due to the specificity of the glucose J-coupling network, the editing efficiency for this method at lower fields (e.g., 3T) needs further investigation, but most likely is not as effective as for the higher fields.

The method presented here also detected co-edited resonances of GSH and NAAG, although the optimization process did not include any attempt to detect these resonances simultaneously. As such, this method may be suboptimal for the detection of these co-edited resonances. If the prospect of simultaneous editing of glucose, GSH, and NAAG is relevant for a specific study, an additional

optimization routine should be carried out to maximize the total signal intensity of all resonances of interest. In addition to signal loss due to chemical shift displacement artifact and a small contribution from co-edited homocarnosine (<5%), additional signal loss occurs due to  $T_2$  relaxation for the TE = 114 ms data acquisition. The estimation of the  $T_2$  relaxation time for  $\beta$ -glc at 3.23 ppm is beyond the scope of this study and, to the best of our knowledge, it has not been measured previously in vivo. The  $T_1$  effect on the signal intensity should be negligible because relatively long TR of 6s was used.

## CONCLUSION

In conclusion, we have presented an optimized homonuclear J-difference editing method, an asymmetric jedit-SLASER sequence, for the quantification of intrinsic glucose concentration. This method does not require glucose injections and  $^{13}\text{C}$  hardware to observe glucose in vivo. The unwanted co-edited homocarnosine contribution is minimal (<5%) at 7T. This method has the potential to provide valuable information on intrinsic glucose concentration in the human brain in vivo. The work presented here also highlights the powerful use of numerical simulations for the purpose of arriving at highly optimized detection of specific metabolites.

## ACKNOWLEDGMENT

The authors are grateful to Dr. Sadato at the National Institute for Physiological Science, Okazaki, Aichi, Japan, for his kind encouragement and support of this research. L.K. wishes to thank Dr. Ben Inglis at University of California, Berkeley, USA, for providing the initial idea to explore glucose detection in vivo at 7T. This project would not be possible without support of Siemens Healthcare KK in Tokyo, Japan, and its R&C Director, Junko Inoue.

## REFERENCES

1. Hertz L, Dienel GA. Energy metabolism in the brain. *Int Rev Neurobiol* 2002;51:1–102.
2. Gruetter R, Novotny EJ, Boulware SD, Rothman DL, Mason GF, Shulman GI, Shulman RG, Tamborlane W V. Direct measurement of brain glucose concentrations in humans by  $^{13}\text{C}$  NMR spectroscopy. *Proc Natl Acad Sci U S A* 1992;89:1109–1112.
3. Walker-Samuel S, Ramasawmy R, Torrealdea F, et al. In vivo imaging of glucose uptake and metabolism in tumors. *Nat Med* 2013;19:1067–1072.
4. Gruetter R, Adriany G, Choi I-Y, Henry P-G, Lei H, Oz G. Localized in vivo  $^{13}\text{C}$  NMR spectroscopy of the brain. *NMR Biomed* 2003;16:313–338.
5. Henry PG, Tkac I, Gruetter R. 1H-localized broadband  $^{13}\text{C}$  NMR spectroscopy of the rat brain in vivo at 9.4 T. *Magn Reson Med* 2003;50:684–692.
6. Gruetter R, Garwood M, Ugurbil K, Seaquist ER. Observation of resolved glucose signals in 1H NMR spectra of the human brain at 4 Tesla. *Magn Reson Med* 1996;36:1–6.
7. Marjanska M, Henry PG, Bolan PJ, Vaughan B, Seaquist ER, Gruetter R, Ugurbil K, Garwood M. Uncovering hidden in vivo resonances using editing based on localized TOCSY. *Magn Reson Med* 2005;53:783–789.
8. Mangia S, Kumar AF, Moheet AA, Roberts RJ, Eberly LE, Seaquist ER, Tkáč I. Neurochemical profile of patients with type 1 diabetes measured by (1)H-MRS at 4 T. *J Cereb Blood Flow Metab* 2013;62440:1–6.
9. de Graaf RA. *In Vivo NMR Spectroscopy: Principles and Techniques*: 2nd Edition. Chichester, UK: John Wiley & Sons; 2007.

10. Gruetter R, Ugurbil K, Seaquist E. Steady-state cerebral glucose concentrations and transport in the human brain. *J Neurochem* 1998;70:397–408.
11. Tkac I, Oz G, Adriany G, Ugurbil K, Gruetter R. In vivo  $^1\text{H}$  NMR spectroscopy of the human brain at high magnetic fields: metabolite quantification at 4T vs 7T. *Magn Reson Med* 2009;62:868–879.
12. Keltner JR, Wald LL, Ledden PJ, Chen YCI, Matthews RT, Kuestermann EH, Baker JR, Rosen BR, Jenkins BG. A localized double-quantum filter for the in vivo detection of brain glucose. *Magn Reson Med* 1998;39:651–656.
13. De Graaf RA, Dijkhuizen RM, Biessels GJ, Braun KP, Nicolay K. In vivo glucose detection by homonuclear spectral editing. *Magn Reson Med* 2000;43:621–626.
14. Mescher M, Merkle H, Kirsch J, Garwood M, Gruetter R. Simultaneous in vivo spectral editing and water suppression. *NMR Biomed* 1998;11:266–272.
15. Oz G, Tkac I. Short-echo, single-shot, full-intensity proton magnetic resonance spectroscopy for neurochemical profiling at 4T: Validation in the cerebellum and brainstem. *Magn Reson Med* 2011;65:901–910.
16. Kelley DA, Wald LL, Star-Lack JM. Lactate detection at 3T: compensating J coupling effects with BASING. *J Magn Reson Imaging* 1999;9:732–737.
17. Govindaraju V, Young K, Maudsley AA. Proton NMR chemical shifts and coupling constants for brain metabolites. *NMR Biomed* 2000;13:129–153.
18. Ernst R, Bodenhausen G, Wokaun A. Principles of nuclear magnetic resonance in one and two dimensions. Oxford, UK: Oxford Science Publications, Oxford University Press; 1987.
19. Allerhand A. Analysis of Carr—Purcell spin-echo NMR experiments on multiple-spin systems. I. The effect of homonuclear coupling. *J Chem Phys* 1966;44:902.
20. Kaiser LG, Young K, Matson GB. Numerical simulations of localized high field  $^1\text{H}$  MR spectroscopy. *J Magn Reson* 2008;195:67–75.
21. Kaiser LG, Young K, Meyerhoff DJ, Mueller SG, Matson GB. A detailed analysis of localized J-difference GABA editing: theoretical and experimental study at 4T. *NMR Biomed* 2008;21:22–32.
22. Marques JP, Kober T, Krueger G, van der Zwaag W, Van de Moortele PF, Gruetter R. MP2RAGE, a self bias-field corrected sequence for improved segmentation and T1-mapping at high field. *Neuroimage* 2010;49:1271–1281.
23. Matson GB. An integrated program for amplitude-modulated RF pulse generation and re-mapping with shaped gradients. *Magn Reson Imaging* 1994;12:1205–1225.
24. Soher BJ, Young K, Kaiser L. Virtual MRS. Spectral simulation and its applications. *Annu Reports NMR Spectrosc* 2010;71:77–102.
25. Veshtort M, Griffin RG. SPINEVOLUTION: A powerful tool for the simulation of solid and liquid state NMR experiments. *J Magn Reson* 2006;178:248–282.
26. Andreychenko A, Boer VO, Arteaga De Castro CS, Luijten PR, Klomp DWJ. Efficient spectral editing at 7T: GABA detection with MEGASLASER. *Magn Reson Med* 2012;68:1018–1025.
27. Roslund MU, Tähtinen P, Niemitz M, Sjöholm R. Complete assignments of the  $^1\text{H}$  and  $^{13}\text{C}$  chemical shifts and JH,H coupling constants in NMR spectra of d-glucopyranose and all d-glucopyranosyl-d-glucopyranosides. *Carbohydr Res* 2008;343:101–112.